SHEAR CAPACITY OF REINFORCED CONCRETE CORBELS USING MECHANISM ANALYSIS

Keun-Hyeok Yang[a], and Ashraf F. Ashour[b]

[a] *Corresponding author, Department of Architectural Engineering, Mokpo National University, Mokpo, Jeonnam, South Korea.*

[b] *EDT1, School of Engineering, Design and Technology, University of Bradford, Bradford, BD7 1DP, U.K.*

Keun-Hyeok Yang is an assistant professor at Mokpo National University, Korea. He received his MSc and PhD degrees from Chungang University, Korea. His research interests include ductility, strengthening and shear of reinforced high-strength concrete structures.

Ashraf F. Ashour is the director of civil engineering at the University of Bradford, UK. He obtained his BSc and MSc degrees from Mansoura University, Egypt and his PhD degree from Cambridge University, UK. His research interests include shear, plasticity and optimisation of reinforced concrete and masonry structures.

ABSTRACT

A mechanism analysis is developed to predict the shear capacity of reinforced concrete corbels. Based on shear failure planes observed in experimental tests, kinematically admissible failure modes are idealized as an assemblage of two rigid blocks separated by failure surface of displacement discontinuity.

Shear capacity predictions obtained from the developed mechanism analysis are in better agreement with corbel test results of a comprehensive database compiled from the available literature than other existing models for corbels. The developed mechanism model shows that the shear capacity of corbels generally decreases with the increase of shear span-to-depth ratio, increases with the increase of main longitudinal reinforcement up to a certain limit beyond which it remains constant, and decreases with the increase of horizontal applied loads. In addition, the smaller the shear span-to-overall depth ratio of corbels, the more effective the horizontal shear reinforcement.

Keywords: corbels, shear capacity, upper-bound theorem, shear-friction theory, strut-and-tie model.

INTRODUCTION

Reinforced concrete corbels, generally defined as short cantilevers having shear span-to-depth ratios less than or equal to 1.0, are commonly used to transfer loads from beams to columns or walls in precast concrete construction. Corbels are primarily designed to resist vertical loads and horizontal actions owing to restrained shrinkage and creep of the supported beam. Due to their geometric proportions, the capacity of reinforced concrete corbels is governed by shear rather than flexure and shear deformations are not negligible, similar to deep beams. Reinforced concrete corbels are identified as discontinuity regions[1] where strain distribution is significantly non-linear and conventional beam theory would not be applicable.

Reinforced concrete corbels are generally known to display several modes of failure[2-4], such as anchorage failure or yielding of main longitudinal reinforcement, shear splitting at the interface between column and corbel, diagonal splitting or crushing of the concrete strut joining the loading point and bottom point of the interface, and local crushing failure under the bearing plate of the applied load. Russo et al.[4], and Yong and Balaguru[5] also identified failure occurring between the interface and diagonal plane joining the loading point and bottom point of the interface as beam-shear failure, the mode of failure mostly observed in experimental tests[5-8]. Premature failure modes,

such as anchorage failure of main longitudinal reinforcement and bearing failure[6], would be prevented by following proper reinforcement detailing as specified in ACI 318-08[9]. However, it is not straightforward to evaluate the capacity of corbels owing to beam-shear failure and crushing of concrete strut as it involves various parameters such as the amount of main longitudinal and horizontal shear reinforcements, shear span-to-depth ratio and amount of horizontal load[5, 7].

In the present study, a mechanism analysis to evaluate the shear capacity of corbels is developed using upper-bound theorem of concrete plasticity. Based on experimental tests carried out by many researchers[5-8, 10], kinematically admissible failure modes are idealized and studied. The effect of different parameters on the shear capacity of corbels is also investigated using the developed mechanism analysis, existing empirical equation by Fattuhi[7], shear-friction model by ACI 318-08[9], simplified strut-and-tie model by Russo et al.[4], softened strut-and-tie model by Hwang et al.[11] and test results of a comprehensive database compiled from available literature.

RESEARCH SIGNIFICANCE

The aim of this paper is to present a mechanism analysis developed from the energy principle for evaluating the shear capacity of reinforced concrete corbels to complement the existing strut and tie approach based on the equilibrium method. The proposed mechanism technique gives closer prediction to test results of 265 corbels than other models available in the literature. The effect of various parameters on the shear capacity of corbels is also evaluated using the developed mechanism analysis, other existing models and experimental results.

REVIEW OF EXISTING MODELS

Currently available theoretical models to evaluate the shear capacity of corbels would be classified into three categories: empirical equations[7] calibrated against test results, formulas[9, 10] developed from shear-friction theory, and strut-and-tie models[4,11,14-16] including plastic truss models[6]. Existing models for estimating the shear capacity of corbels are summarized below.

Empirical equation

Based on extensive test results, Fattuhi[7] combined different parameters influencing the shear capacity V_n of corbels and developed the following formula:

$$V_n = k_1(bd)^{k_2}(f_{ct})^{k_3}(a/d)^{k_4}(\rho_{st})^{k_5}(10)^{k_6(N/V)}(f_y/f_{cu})^{k_7}(d/h)^{k_8} \quad (1)$$

where b, d and h (in mm) = width, effective depth, and overall depth of the interface between column and corbel, respectively, a = shear span measured from the loading point to the interface as shown in Fig. 1, f_{ct} (in MPa) = indirect tensile splitting strength of concrete, f_{cu} = cube compressive strength of concrete (≅1.23 f_c', where f_c' = cylinder compressive strength), $\rho_{st}\left(=\frac{A_{st}}{bd}\right)$ = ratio of main longitudinal reinforcement, A_{st} and f_y = area and yield point stress of main longitudinal reinforcement, respectively, and V and N = vertical and horizontal loads applied to corbels, respectively. The values of the constants k_1 to k_8 obtained from regression analysis[7] of test data are 611, 0.7298, 0.3569, -0.8204, 0.5745, -0.1644, -0.0261, -0.1342, respectively. The above equation takes no account of the influence of horizontal shear reinforcement.

Although it is relatively easy to use empirical equations such as Eq. (1), its application to corbels having parameters deviated from the range used for calibration is doubtful. In addition, this equation may cause overfitting due to the high number of constants used to develop the equation.

Formula using shear-friction theory

ACI 318-08[9] specifies the shear capacity of corbels considering the load transfer capacity of horizontal reinforcement by shear friction and flexural yielding of the main longitudinal reinforcement at the interface as follows:

$$V_n = \min\left[\mu\left(A_{st}f_y + A_h f_{yh}\right), \frac{A_{st}f_y jd - N(h-d+jd)}{a}\right] \le \min\left(0.2f_c'bd, 5.5bd\right) \quad (2a)$$

$$V_n = \min\left[\mu\left(A_{st} f_y + A_h f_{yh} - N\right), \frac{A_{st} f_y jd - N\left(h - d + jd\right)}{a}\right] \le \min\left(0.2 f_c' bd, 5.5bd\right) \quad (2b)$$

where μ = coefficient of friction which is taken as 1.4 for monolithic construction, A_h and f_{yh} = total area and yield strength of horizontal shear reinforcement, and $jd\left[= d - 0.5\left(A_{st} f_y - N\right)/\left(0.85 f_c' b\right)\right]$= moment lever arm.

The above formula based on shear-friction theory neglects the shear transfer capacity of concrete as the critical failure section is always assumed at the interface between corbel and column as shown in Fig. 1. However, failure of corbels having a very small shear span-to-depth ratio or sufficient horizontal shear reinforcement seldom occurs along the interface as pointed out by Hwang et al.[11] and Hermansen and Cowan[12]. In addition, ACI 318-08 limits concrete strength of corbels to $f_c' \le 27.5$ MPa (3.99 ksi) when the shear capacity of corbels is governed by the second part of Eq. (2), which does not allow full utilisation of higher strength concrete. For corbels having shear span to depth ratio greater than 1.0, ACI 318-08 recommends the use of strut and tie model described in ACI 318-08, Appendix A.

Strut-and-tie model

Considering equilibrium, compatibility and constitutive laws of cracked reinforced concrete, Hwang et al.[11] predicted the shear capacity of corbels based on the softened strut-and-tie model shown in Fig. 2(a) as follows:

$$V_n = -F_D \sin\theta + F_h \tan\theta \quad (3)$$

where F_D and F_h = compression force in concrete strut and tension force in the horizontal shear reinforcement, respectively, $\theta\left(= \tan^{-1}\frac{jd_1}{a}\right)$ = angle of concrete strut to the longitudinal axis of corbels as shown in Fig. 2 (a). Hwang et al. used the linear bending theory of reinforced concrete

beams with only tensile reinforcement neglecting shear deformations and the non-linear distributions of strains and stresses of corbels to estimate the moment lever arm jd_1 as:

$$jd_1 = \left(1 - \frac{k}{3}\right)d \tag{4}$$

where $k\left(= \sqrt{(n\rho_f)^2 + 2n\rho_f} - n\rho_f\right)$ = ratio of depth of compression zone to the effective depth at the interface, $\rho_f\left(= \frac{A_{st} - A_n}{bd}\right)$ = equivalent main longitudinal reinforcement ratio, $A_n\left(= \frac{N}{f_y}\right)$ = area of main longitudinal reinforcement resisting the applied horizontal force N, $n\left(= \frac{E_s}{E_c}\right)$ = modular ratio of elasticity, E_s and $E_c\left(= 4700\sqrt{f_c'}\ \text{in MPa}\right)$ = elastic moduli of reinforcement and concrete, respectively. In Eq. (3), F_h is assumed to be a function of the area A_h and average strain of horizontal shear reinforcement, and F_D is dependent on the concrete strut width w_s assumed to be equal to kd, angle θ and maximum allowable compressive stress $\sigma_{d,\max}$ of concrete strut. Hwang et al. adopted the softened stress-strain curve of cracked concrete proposed by Zhang and Hsu[13] to estimate $\sigma_{d,\max}$ that is depending on the average principal compressive ε_d and tensile ε_r strains in concrete and a softening coefficient ξ.

The compatibility condition considered by Hwang et al. relates the average principal strains to the average horizontal ε_h and vertical ε_v strains as below:

$$\varepsilon_r + \varepsilon_d = \varepsilon_h + \varepsilon_v \tag{5}$$

To avoid iterative procedure, Hwang et al. proposed reasonable values for the average horizontal ε_h and vertical ε_v strains and hence, the values of ε_d and ε_r can be determined using numerical analysis. As a result, the shear capacity of corbels using the softened strut-and-tie model proposed

by Hwang et al can be obtained, though several assumptions based on linear elastic beam theory are imposed.

On the other hand, Russo et al.[4] derived a simple equation using the strut-and-tie model shown in Fig. 2(b). In this model, load transfer mechanisms of cracked concrete and horizontal shear reinforcement were considered and simplified as below:

$$V_n = 0.8\left(k\chi f_c^{'} \cos\theta_1 + 0.65\rho_h f_{yh} \cot\theta_1\right)bd \tag{6}$$

where χ = a nondimensional interpolating function to provide a single expression for softening coefficient ξ given in the softened strut-and-tie model above, θ_1 = angle of concrete strut to the column axis as shown in Fig. 2 (b), which can be obtained from the elastic beam theory and trigonometric relations, and $\rho_h \left(= \frac{A_h}{bd} \right)$ = ratio of horizontal shear reinforcement. The principal tensile strain ε_r was assumed to be f_{ct} / E_c to obtain directly the softening coefficient ξ. Russo et al. also proposed that χ could be approximately expressed as a polynomial of third degree in $f_c^{'}$. Different constants used in Eq. (6) were determined by calibrating the strut-and-tie model against 243 test results of corbels.

Other strut and tie models[14-16] were developed for corbels but they are similar in principle to those presented above. Strut-and-tie models provide a systematic load transfer mechanism for estimating the shear capacity of corbels. However, they consider only the failure mode due to crushing of concrete struts. In addition, several assumptions are imposed for simplification. The width and inclination of concrete strut is evaluated from the neutral axis depth of the interface using the conventional elastic beam theory that is not applicable to deep corbels where both strains and stresses are non linear. In addition, biaxial stresses in compressed concrete strut are chosen arbitrarily or calculated from tensile strength of concrete.

MECHANISM ANALYSIS

Failure mechanism of corbels

Failure planes of corbels commonly occurred along the diagonal plane joining the inner edge of loading plate and bottom point of the interface[2, 3]. However, few test specimens exhibited splitting cracks stemmed from a point close to the loading plate at failure[2, 3]. Thus, the failure mechanism can be idealized as an assemblage of two rigid blocks separated by a yield line representing the failure zone along which in-plane displacement discontinuity occurs[17]. Rigid block *I* undergoes a rotation around an instantaneous center (I.C.), while rigid block *II* is considered to be fixed with the supporting column as shown in Fig. 3. I.C. can be located anywhere in the vertical plane of corbel and its position identifies the shape of the failure surface. Jensen[18] proved that the optimal shape of the yield line is a hyperbola with orthogonal asymptotes at the I.C. and the yield line reduces to a straight line to achieve a stationary value of the total energy dissipation when the I.C. approaches infinity. On the other hand, the yield line turns into two straight segments when the I.C. of relative rotation lies inside or on a circle whose diameter is the straight yield line joining the inner edge of loading plate and bottom point of the interface as shown in Fig. 3 (b). For each location of I.C., an upper bound load to the corbel capacity can be established. However, the optimum position of I.C. corresponds to the minimum load capacity as explained below.

Material Modelling

Concrete is assumed to be a rigid perfectly plastic material obeying the modified Coulomb failure criteria[17] with zero tension cut-off. The effective compressive strength to be used in calculation, f_c^*, is

$$f_c^* = \nu_e f_c' \tag{7}$$

where ν_e = effectiveness factor that is introduced to account for the limited ductility of concrete and to absorb other shortcomings of applying the plasticity theory to concrete. Although there is no unified approach for evaluating the effectiveness factor of concrete, many investigations[19, 20] clearly showed that the effectiveness factor depends on concrete strength and geometrical properties of reinforced concrete members. The measure of success of the mechanism analysis presented below would depend on the extent that the effectiveness factor is reasonably uniform and predictable across the range of corbels considered. In the present study, Nielsen's model[17] considering the effect of compressive strength of concrete modified by the equation proposed by Bræstrup[20] for the influence of shear span-to-overall depth ratio is adopted for the evaluation of the effectiveness factor as given below:

$$\nu_e = \left(0.8 - \frac{f_c^{'}}{200}\right)\left(1 - 0.2\frac{a}{h}\right) \tag{8}$$

All reinforcement is considered to carry only axial tensile and compressive stresses and its dowel action is ignored. Steel reinforcement in both tension and compression is assumed to be a rigid perfectly plastic material with yield strength f_y. Yielding of steel reinforcements is generally achieved by utilizing some sort of a mechanical anchorage at the end of the corbel. Strain hardening of steel reinforcement is ignored as it requires excessive wide cracks in concrete beyond the failure mechanism considered in the present analysis.

Work Equation

The upper-bound theorem is based on the energy principle, by equating the total internal energy, W_I, to the external work done, W_E. The total internal energy mainly depends on the position of the I.C. and the amount of internal stresses in both concrete along the yield line and reinforcement

crossing the yield line. The energy $(W_c)_l$ dissipated in concrete per unit length of the yield line is written in the following general form[17]:

$$(W_c)_l = \frac{\nu_e f_c^{'}}{2} b\delta(1-\sin\alpha) \tag{9}$$

where δ = relative displacement rate of rigid block *I* and α = angle between the relative displacement at the midpoint of the chord and yield line chord as shown in Fig. 3. The relative displacement rate δ can be expressed as $\omega \cdot r$, where r = distance between the midpoint of the chord of the yield line and the I.C. and ω = rotational displacement of rigid block *I*. For a yield line with two straight segments as shown in Fig. 3 (b), it should be noted that the two segments intersect at the I.C. of relative rotation, indicating that one segment of the yield line is under compression and the other is in tension due to the relative rotation between the two blocks. Therefore, one segment of the yield line is under tensile stresses with pure separation ($\alpha = \frac{\pi}{2}$), and it can not contribute to the internal energy distribution due to the assumption of zero tensile concrete strength. If the origin of global coordinates is set to be at the bottom point of the interface as shown in Fig. 3, the total internal energy W_c dissipated in concrete along the hyperbolic or two straight yield line is[18]:

$$W_c = \frac{\nu_e f_c^{'}}{2} b\omega F(O') \tag{10}$$

where $F(O')$ is a function of the position of the I.C. and, consequently, the shape of the yield line; Eqs. 11(a) and 11(b) below gives the value of $F(O')$ for the hyperbolic and two straight segments yield lines respectively[18].

$$F(O') = r(1-\sin\alpha)h/\sin\beta \qquad \text{for} \qquad r > h/(2\sin\beta) \tag{11a}$$

$$F(O') = \left(X_{ic}^{\ 2} + Y_{ic}^{\ 2}\right) \qquad \text{for} \qquad r \le h/(2\sin\beta) \tag{11b}$$

where $\beta = \left(\tan^{-1}(h/x_e)\right)$= angle of the diagonal line joining the inner edge of the loading plate and bottom point of the interface to the longitudinal axis of corbels and x_e = clear shear span measured

from inner edge of the loading plate to interface. In Eq. (11 a), both r and α depend on the position of the I.C. Hence, the energy dissipated in concrete is a function of horizontal X_{ic} and vertical Y_{ic} coordinates of the I.C.

The relative displacement of reinforcement δ_s can be expressed as $\omega \cdot r_s$ as shown in Fig. 4. Therefore the energy W_s dissipated in main longitudinal and web reinforcement crossing the yield line is calculated from:

$$W_s = \sum_{i=1}^{n} \omega (A_s)_i (f_y)_i (r_s)_i \cos(\alpha_s)_i \tag{12}$$

where n = number of reinforcing bars crossing the yield line, $(A_s)_i$ and $(f_y)_i$ = area and yield strength of reinforcing bar i crossing the yield line, respectively, $(r_s)_i$ = distance between the intersection point of reinforcing bar i with the yield line and the I.C. and $(\alpha_s)_i$ = angle between the relative displacement $(\delta_s)_i$ and the reinforcing bar i crossing the yield line. In case of horizontal reinforcement, $\cos(\alpha_s)_i = |Y_{ic} - y_i| / (r_s)_i$, where y_i = vertical coordinate of the intersection point of reinforcing bar i and the yield line as shown in Fig. 4.

The external work W_E done by the vertical load V_n and horizontal load N on rigid block I is (see Fig. 3):

$$W_E = V_n \omega |a - X_{ic}| + N\omega |h - Y_{ic}| \tag{13}$$

In Eq. (13) above, the horizontal load N is assumed to act at the level of the corbel top surface. However, this could be easily adjusted to other levels as the case in some experiments[5, 7]. The horizontal load N applied to corbels can be normalized with respect to the yielding force, $A_{st}\, f_y$, of the main longitudinal reinforcement to simplify the calculation of the vertical coordinate Y_{ic} of the I.C. Equating the total internal energy dissipated in concrete and reinforcement to the external work done, the shear capacity, V_n, can be obtained as below:

$$V_n = \frac{bhf_c^{'}}{|a - X_{ic}|}\left[\frac{\nu_e}{2h}F(O^{'}) + \phi_{st}\left(|d - Y_{ic}| - \lambda|h - Y_{ic}|\right) + \sum_{i=1}^{n}(\phi_s)_i (r_s)_i \cos(\alpha_s)_i\right] \quad (14)$$

where $\phi_{st} = \frac{A_{st} f_y}{bhf_c^{'}}$ = main longitudinal reinforcement index, $\lambda\left(= \frac{N}{A_{st} f_y}\right)$ = ratio of horizontal load to the yield force of the main longitudinal reinforcement, and $(\phi_s)_i = \frac{(A_s)_i (f_y)_i}{bhf_c^{'}}$ = web reinforcement index for each individual reinforcing bar *i* crossing the yield line. Eq. (14) implies that the horizontal load is one of various parameters influencing the vertical coordinate Y_{ic} of the I.C.

Solution procedure

According to the upper-bound theorem, the collapse occurs at the least strength. The shear capacity of corbels is implicitly expressed as a function of the position of the I.C., (X_{ic}, Y_{ic}), as given by Eq. (14). The horizontal X_{ic} and vertical Y_{ic} coordinates of the I.C. is repeatedly tuned until the minimum shear capacity is obtained. For each position of the I.C., the shape of the yield line can be identified, the energy dissipated in concrete along the yield line can be estimated using Eqs. 10 and 11(a) or Eqs. 10 and 11(b) for the hyperbolic and two straight segments yield lines, respectively and finally the corresponding shear capacity is calculated using Eq. (14). The process of adjusting the position of I.C. is achieved by reliable numerical optimization procedures provided in MATLAB software. However, if such routines are not available, a simple algorithm has to be developed to survey a wide range of locations of I.C. to achieve the minimum load capacity of corbel.

Ashour[22] developed a mechanism analysis for reinforced concrete deep beams and showed that the position of the I.C. of relative rotation commonly depends on the amount of main longitudinal reinforcement and shear span-to-overall depth ratio. The two straight yield lines clearly indicate yielding and participation of the main longitudinal top reinforcement of corbels, whereas in case of

the hyperbolic yield line, the I.C. is more likely to be located along the main longitudinal top reinforcements and consequently, these reinforcements do not contribute to the internal energy dissipation. For the case of corbels, the position of the I.C. would also be influenced by the amount of the applied horizontal force.

When shear reinforcement is not provided in concrete corbels, the determination of the minimum shear capacity could be achieved by considering the two differential equations, $\frac{\partial V_n}{\partial X_{ic}} = 0$ and $\frac{\partial V_n}{\partial Y_{ic}} = 0$. In addition, for corbels with sufficiently strong main longitudinal reinforcement or subjected to high horizontal load *N*, the vertical coordinate Y_{ic} of the I.C. would be located at the level of main longitudinal reinforcement[22] or horizontal applied load. As a result, the optimization process is further simplified as the shear capacity turns to be a function of only X_{ic}. A numerical example explaining the solution procedure of shear capacity calculation of specimen PA 2 tested by Foster et al.[8] using the mechanism approach is presented in Appendix A.

COMPARISONS AND DISCUSSIONS

Database of reinforced concrete corbels

Test results of 265 reinforced concrete corbels were compiled from different experimental investigations carried out by Abdul-Wahab[23], Campione et al.[6], Chakrabarti et al.[24], Fattuhi et al.[7, 25-29], Foster et al.[8] Kriz and Raths[3], Mattock et al.[30], and Yong and Balaguru[5], and other test results originally collected by Kriz and Raths[3]. All corbels were reported to fail in shear due to a major diagonal crack within the corbel shear span. The test specimens were made of concrete having a relatively low compressive strength of 15.2 MPa (2.2 ksi) and very high compressive strength of 105 MPa (15.2 ksi). The shear span-to-overall depth ratio of corbels ranged from 0.1 to 1.1. The

main longitudinal reinforcement index ϕ_{st} varied between 0.023 and 0.487 whereas the horizontal load to yield force of main longitudinal reinforcement ratio $\lambda\left(=\frac{N}{A_{st}f_y}\right)$ ranged from 0 to 1.0. Some test specimens had no shear reinforcement whereas others were reinforced with horizontal shear reinforcement only. However, all test specimens had no vertical shear reinforcement.

Comparison of shear load capacity

Table 1 gives the mean $\gamma_{cs,m}$, standard deviation $\gamma_{cs,s}$, and coefficient of variation $\gamma_{cs,v}$ of the ratio between measured and predicted shear capacities, $\gamma_{cs}=(V_n)_{Exp.}/(V_n)_{\mathrm{Pre.}}$, of corbels with different horizontal shear reinforcement and horizontal load. The distribution of γ_{cs} of the total specimens in the database against the shear span-to-overall depth ratio a/h is also shown in Fig. 5; Fig. 5 (a) for the empirical equation (Eq. (1)) proposed by Fattuhi, Fig. 5 (b) for the ACI 318-08 equation (Eq. (2)) based on shear-friction theory, Fig. 5 (c) for the simplified softened strut-and-tie model proposed by Hwang et al., Fig. 5 (d) for the strut-and-tie model by Russo et al., and Fig. 5 (e) for the current mechanism analysis. Fattuhi's equation largely overestimates the shear capacity of corbels without both horizontal shear reinforcement and horizontal load when $a/h \leq 0.3$, whereas underestimates that of corbels with horizontal shear reinforcement and without horizontal load regardless of a/h, as the contribution of horizontal shear reinforcement to shear transfer capacity is not included in this method. The largest standard deviation and coefficient of variation of all models appears in the equations specified in ACI 318-08 based on the shear-friction theory. In particular, the ACI 318-08 equations are unconservative for corbels without horizontal shear reinforcement. The softened strut-and-tie model proposed by Hwang et al. generally underestimates the shear capacity of corbels, especially those without both horizontal shear reinforcement and horizontal load. Russo et al.'s strut-and-tie model shows reasonable agreement with test results, but high deviation

exhibited by few specimens without horizontal shear reinforcement or with horizontal load as shown in Fig. 5 (d). On the other hand, predictions obtained from the developed mechanism analysis are in better agreement with test results than other models regardless of shear span-to-overall depth ratio, horizontal shear reinforcement and horizontal load, as given in Table 1.

FURTHER EXPERIMENTAL VERIFICATION

The influence of various parameters on the shear capacity of corbels is evaluated using the empirical equations proposed by Fattuhi, the equation specified in ACI 318-08 based on shear-friction theory (SFT), strut-and-tie models (STM) developed by Hwang et al. and Russo et al., the current mechanism analysis, and appropriate experimental results in the database. In this parametric study, the width and overall depth of section in the interface between columns and corbels, and compressive strength of concrete are selected to be fixed at 150 mm (5.9 in.), 600 mm (23.6 in.), and 30 MPa (4.35 ksi), respectively. The effective depth of section and width of loading plate are also assumed to be $0.9\,h$ and $0.1\,h$, respectively. In addition, the shear capacity of corbels is normalized by $bhf_c^{'}$. In few cases, when a value of corbel parameter used in the parametric study is not matching that in the database, a range of such parameter is extracted from the database and presented in the following figures to validate the trend predicted by different theoretical models.

Shear span-to-overall depth ratio

Fig. 6 shows the influence of the shear span to depth ratio a/h on the normalized shear capacity $V_n/bhf_c^{'}$ of corbels without both horizontal shear reinforcement and horizontal load. Calculations obtained from ACI 318-08 remain constant when $a/h \leq 0.6$ as the shear-friction theory considers only the shear transfer of reinforcement crossing the failure plane at the interface, independent of a/h. On the other hand, normalized shear capacities of corbels obtained from experimental results, empirical equations, strut-and-tie models and mechanism analysis generally decrease with the

increase of a/h. However, the strut-and-tie models gives higher predictions than mechanism analysis, empirical equation, and experimental results when $a/h \geq 0.5$, especially for $\phi_{st} = 0.05$. In addition, most models, but the mechanism approach and the empirical equation by Fattuhi, underestimate the normalized shear capacity for low shear span to depth ratio (a/h < 0.3), especially for ϕ_{st} = 0.1.

Main longitudinal reinforcement

The influence of the main longitudinal reinforcement index ϕ_{st} on the normalized shear capacity $V_n / bhf_c^{'}$ of corbels without horizontal shear reinforcement and horizontal load for two different shear span-to-overall depth ratios is presented in Fig. 7. The prediction obtained from the mechanism analysis increases with the increase of ϕ_{st} up to a certain limit beyond which the normalized shear capacity remains constant, agreeing with the test results. When the main longitudinal reinforcement reaches this limit, it becomes strong enough not to yield and hence the I.C. lies at the level of the main longitudinal reinforcement. In this case, the main longitudinal reinforcement would have no contribution to the shear capacity of corbels as depicted in Fig. 7. The shear capacity predicted from ACI 318-08 is governed by the upper limit specified by Eq. (2) with the increase of ϕ_{st}. For the mechanism analysis and ACI 318-08, the limit to the ϕ_{st} depends on a/h, indicating that the value of ϕ_{st} to achieve the peak point decreases with the decrease of a/h. On the other hand, the prediction obtained from empirical equation, and strut-and-tie models increases with the increase of ϕ_{st} without any limits, exhibiting large overestimation of test results for large ϕ_{st}, especially for a/h=0.9.

Horizontal load

Fig. 8 shows the effect of the ratio λ of the applied horizontal load to yield force of main longitudinal reinforcement on normalized shear capacity $V_n / bhf_c^{'}$ of corbels without horizontal shear reinforcement for two different shear span to overall depth ratios a/h. The normalized shear capacity of corbels steadily decreases with the increase of λ as predicted by all theoretical models and experimental results. However, the predictions obtained from the mechanism analysis are closer to the experimental results than other models. In particular, strut-and-tie models largely overestimate the effect of λ on the normalised shear capacity for a/h = 0.5.

Horizontal shear reinforcement

The effect of horizontal shear reinforcement index $\phi_h \left(= \frac{A_h f_{yh}}{bhf_c^{'}} \right)$ on the normalized shear capacity $V_n / bhf_c^{'}$ of corbels without horizontal load is shown in Fig. 9. The normalized shear capacity of corbels increases with the increase of ϕ_h as predicted by the mechanism analysis and strut-and-tie models and also supported by the limited experimental results available. The effect of horizontal shear reinforcement on the shear capacity of corbels is more prominent in low a/h, namely, a higher increasing rate is developed in corbels with a/h of 0.3 than corbels with a/h of 0.9. However, prediction obtained from Fattuhi's equations does not account for ϕ_h, and the ACI 318-08 prediction is also independent of ϕ_h for a/h = 0.9 and slightly increases with the increase of ϕ_h for a/h=0.3.

CONCLUSIONS

A mechanism analysis based on upper-bound theorem is proposed to predict the shear capacity of reinforced concrete corbels. The effect of different parameters on the shear capacity of corbels is also investigated using the developed mechanism analysis, empirical equations proposed by Fattuhi, ACI 318-08 based on shear-friction theory, strut-and-tie models developed by Hwang et al. and Russo et al., and test results in a comprehensive database collected from the available literature. The following conclusions may be drawn:

1. Compared with the existing models, predictions obtained from the developed mechanism analysis are in better agreement with test results regardless of shear span-to-overall depth ratio, horizontal shear reinforcement and horizontal load.
2. The largest standard deviation and coefficient of variation of the ratio between measured and predicted shear capacities of corbels are shown by ACI 318-08. In addition, ACI 318-08 is unconservative for corbels having shear span-to-overall depth ratio more than 0.5.
3. The normalized shear capacities $V_n / bhf_c^{'}$ of corbels obtained from experimental results, empirical equations, strut-and-tie models and mechanism analysis generally decrease with the increase of shear span-to-overall depth ratio.
4. The shear capacity obtained from the mechanism analysis increases with the increase of the main longitudinal reinforcement index up to a certain value beyond which it remains constant, agreeing with test results.
5. The normalized shear capacity $V_n / bhf_c^{'}$ of corbels deceases with the increase of the horizontal load; the decreasing rate obtained from the mechanism analysis is similar to that of test results.
6. The effect of horizontal shear reinforcement on shear capacity is more prominent in corbels having small shear span-to-overall depth ratios.

ACKNOWLEDGMENTS

This work was supported by the National Research Institute of Cultural Heritage and the Regional Research Centers Program (Bio-housing Research Institute), granted by the Korean Ministry of Education & Human Resources Development.

REFERENCES

1. MacGregor, J. G., Reinforced Concrete : Mechanics and Design, Prentice-Hall International, Inc., 1997.

2. ASCE-ACI Joint Task Committee 426., "The Shear Strength of Reinforced Concrete Members," ASCE Proceedings, V. 99, ST 6, 1973, pp. 1091-1187.

3. Kriz, L. B., and Raths, C. H., "Connections in Precast Concrete Structures-Strength of Corbels," PCI Journal, V. 10, No. 1, 1965, pp. 16-61.

4. Russo, G., Venir, R., Pauletta, M., and Somma, G., "Reinforced Concrete Corbels-Shear Strength Model and Design Formula," ACI Structural Journal, V. 103, No. 1, 2006, pp. 3-10.

5. Yong, Y. K., and Balaguru, P., "Behavior of Reinforced High-Strength-Concrete Corbels," Journal of Structural Engineering, ASCE, V. 120, No. 4, 1994, pp. 1182-1201.

6. Campione, G., Mendola, L. L., and Mangiavillano, M. L., "Steel Fiber-Reinforced Concrete Corbels: Experimental Behavior and Shear Strength Prediction," ACI Structural Journal, V. 104, No. 5, 2007, pp. 570-579.

7. Fattuhi, N. I., "Reinforced Corbels Made with Plain and Fibrous Concretes," ACI Structural Journal, V. 91, No. 5, 1994, pp. 530-536.

8. Foster, S. J., Powell, R. E., and Selim, H. S., "Performance of High-Strength Concrete Corbels," ACI Structural Journal, V. 93, No. 5, 1996, pp. 555-563.

9. ACI Committee 318, Building Code Requirements for Structural Concrete (ACI 318-08) and Commentary (ACI 318R-08). American Concrete Institute, 2008.

10. Mattock, A. H., "Design Proposals for Reinforced Concrete Corbels," PCI Journal, V. 21, No. 3, 1976, pp. 18-42.

11. Hwang, S. J., Lu, W. Y., and Lee, H. J., "Shear Strength Prediction for Reinforced Concrete Corbels," ACI Structural Journal, V. 97, No. 4, 2000, pp. 543-552.

12. Hermansen, B. R., and Cowan, J., "Modified Shear-Friction Theory for Bracket Design," ACI Journal, Proceedings, V. 71, No. 7, 1974, pp. 55-60.

13. Zhang, L. X. B., and Hsu, T. T. C., "Behavior and Analysis of 100 MPa Concrete Membrane Elements," Journal of Structural Engineering, ASCE, V. 124, No. 1, 1998, pp. 24-34.

14. Solanki, H., and Sabnis, G. M., "Reinforced Concrete Corbels-Simplified," ACI Structural Journal, V. 84, No. 5, 1987, pp. 428-432.

15. Hagberg, T., "Design of Concrete Brackets: On the Application of the Truss Analogy," *ACI Structural Journal*, V. 80, No. 1, 1983, pp. 3-12.

16. Siao, W. B., "Shear Strength of Short Reinforced Concrete Walls, Corbels, and Deep Beams," ACI Structural Journal, V. 91, No. 2, 1994, pp. 123-132.

17. Nielsen M. P., Limit Analysis and Concrete Plasticity, Prentice-Hall, Englewood Cliffs, 1984.

18. Jensen, J. F., "Discussion of 'An Upper-Bound Rigid-Plastic Solution for the Shear Failure of Concrete Beams without Shear Reinforcement' by K. O. Kemp and M. T. Al-Safi," Magazine of Concrete Research, V. 34, No. 119, 1982, pp. 100-103.

19. Ashour, A. F., and Morley, C. T., "Effectiveness Factor of Concrete in Continuous Deep Beams," Journal of Structural Engineering, ASCE, V. 122, No. 2, 1996, pp. 169-178.

20. Bræstrup, M. W., Shear Strength Prediction-Plastic Method. Reinforced Concrete Deep Beams, F. K. Kong, ed., Blackie and Son Ltd., 1990, pp. 182-203.

21. Chapman, S. J., MATLAB Programming for Engineers, Thomson, USA, 2004.

22. Ashour, A. F., “Shear Capacity of Reinforced Concrete Deep Beams,” Journal of Structural Engineering, ASCE, V. 126, No. 9, 2000, pp. 1045-1052.

23. Abdul-Wahab, H. M. S., “Strength of Reinforced Concrete Corbels with Fibers,” ACI Structural Journal, V. 86, No. 1, 1989, pp. 60-66.

24. Chakrabarti, P. R., Farahani, D. J., and Kashou, S. I., “Reinforced and Precompressed Concrete Corbels-An Experimental Study,” ACI Structural Journal, V. 86, No. 4, 1989, pp. 405-412.

25. Fattuhi, N. I., “Strength of SFRC Corbels Subjected to Vertical Load,” Journal of Structural Engineering, ASCE, V. 116, No. 3, 1990, pp. 701-717.

26. Fattuhi, N. I., “Strength of FRC Corbels in Flexure,” Journal of Structural Engineering, ASCE, V. 120, No. 2, 1994, pp. 360-377.

27. Fattuhi, N. I., and Hughes, B. P., “Reinforced Steel Fiber Concrete Corbels with Various Shear Span-to-Depth Ratio,” ACI Materials Journal, V. 86, No. 6, 1989, pp. 590-596.

28. Fattuhi, N. I., and Hughes, B. P., “Ductility of Reinforced Concrete Corbels Containing either Steel Fiber or Stirrups,” ACI Structural Journal, V. 86, No. 6, 1989, pp. 644-651.

29. Fattuhi, N. I., “Reinforced Corbels Made with High-Strength Concrete and Various Secondary Reinforcements,” ACI Structural Journal, V. 91, No. 4, 1994, pp. 376-383.

30. Mattock, A. H., Chen, K. C., and Soongswang, K., “The Behavior of Reinforced Concrete Corbels,” PCI Journal, V. 21, No. 2, 1976, pp. 52-77.

Appendix A: Numerical Example of Mechanism Analysis

The following numerical example presents the shear capacity calculation of specimen PA 2 tested by Foster et al.[8] using the mechanism approach. The material and geometrical properties of the specimen PA 2 are as follows: b =150 mm, h =600 mm, $f_c^{'}$ =53 MPa, d =500 mm, a =300 mm, x_e = 250 mm, A_{st} =1884 mm^2 (Y20), f_y =450 MPa, A_h = 157 mm^2 (R10) f_{yh} =360 MPa, and

s_h =85 mm. There was no horizontal load applied to the specimen. The measured shear capacity V_n was 800 kN. The following steps summarise the procedure:

- Calculate the effectiveness factor for concrete ν_e using Eq. (8); ν_e =0.4815.
- Calculate the main longitudinal reinforcement index $\phi_{st} = \frac{A_{st} f_y}{bhf_c^{'}}$ and the web reinforcement index $(\phi_s)_i = \frac{A_h f_{yh}}{bhf_c^{'}}$ for each individual bar crossing the yield line; ϕ_{st} =0.1777, $(\phi_s)_i$ =0.0118.
- Determine the angle $\beta = \left(\tan^{-1}(h/x_e)\right)$ of the diagonal line joining the inner edge of the loading plate and bottom point of the interface to the longitudinal axis of the corbel; β = 67.38deg.
- Different positions of the I.C. (X_{ic}, Y_{ic}) have to be examined using the MATLAB software optimizer[21]. For each position, the shape of the yield line has to be identified using Eq. 11. The internal energy dissipated in concrete has to be estimated using Eqs. 10 and 11. For example, for $X_{ic} = 150mm$ and $Y_{ic} = 150mm$, $r = 152$ mm and $h/(2\sin\beta)$ = 325 mm, ($r \le h/(2\sin\beta)$), the yield line is then identified to be two straight segments and $F(O')$ is then obtained from Eq. (11b), $F(O')$ = 45000 mm^2; however for X_{ic} = 400mm and Y_{ic} = 500mm , r = 340 mm ($r > h/(2\sin\beta)$), the hyperbolic yield line occurred and $F(O')$ is then obtained from Eq. (11 a) as $F(O')$=32273 mm^2.
- The minimum shear capacity V_n of 784 kN is achieved when X_{ic} =1950 mm and Y_{ic} =500 mm (i.e. along the main longitudinal reinforcement). This indicates that the main longitudinal reinforcement does not yield at failure. The predicted shear capacity is 98% of the measured shear failure load.
- Table A.1 compares the shear capacity and location of I.C. of corbels PA1 and PA2 tested by Foster et al.[8] as predicted by the mechanism analysis. Corbel PA1 was a control specimen having the same geometrical dimensions and concrete strength as corbel PA2, but no secondary

horizontal shear reinforcement. The optimum location of I.C. is moved to X_{ic} =496 mm and Y_{ic} =500 mm and the predicted shear capacity is reduced to 596 kN for corbel PA1 (108% of the measured shear capacity). Table A.1 also indicates that a 32% shear capacity increase owing to the use of secondary horizontal shear reinforcement of R10 at spacing of 85mm is predicted using the mechanism analysis.

(Note: 1 MPa = 145 psi; 1 kN = 0.2248 kips; 1 mm = 0.039 in.)

TABLES and FIGURES

List of Tables:

List of Figures:

Table 1-Comparison of experimental and predicted shear capacities of corbels in the database using different methods.

	Fattuhi (Empirical equation)					ACI 318-05 (Shear-friction theory)					Hwang et al. (Softened strut-and-tie model)					Russo et al. (Strut-and-tie model)					This study (Mechanism analysis)				
	W/O	W/H	W/N	W/HN	Total	W/O	W/H	W/N	W/HN	Total	W/O	W/H	W/N	W/HN	Total	W/O	W/H	W/N	W/HN	Total	W/O	W/H	W/N	W/HN	Total
$\gamma_{cs,m}$	0.83	1.23	0.86	0.50	0.86	1.43	1.67	1.07	1.32	1.41	1.16	1.17	1.02	1.07	1.14	1.0	1.02	0.89	0.89	0.98	1.03	0.96	1.05	0.96	1.01
$\gamma_{cs,s}$	0.26	0.24	0.21	0.15	0.31	0.57	0.48	0.24	0.35	0.53	0.27	0.15	0.37	0.26	0.27	0.24	0.19	0.32	0.25	0.25	0.22	0.18	0.22	0.19	0.21
$\gamma_{cs,v}$	0.31	0.19	0.25	0.29	0.36	0.4	0.28	0.23	0.27	0.34	0.23	0.13	0.36	0.25	0.24	0.24	0.18	0.36	0.28	0.25	0.21	0.19	0.21	0.19	0.21

Note : $\gamma_{cs,m}$, $\gamma_{cs,s}$, and $\gamma_{cs,v}$ indicate the mean, standard deviation and coefficient of variation of $\gamma_{cs} = (V_n)_{Exp.}/(V_n)_{Pre.}$, respectively.

W/O, W/H, W/N, and W/HN refer to corbels without both horizontal shear reinforcement and horizontal load, with horizontal shear reinforcement and without horizontal load, without horizontal shear reinforcement and with horizontal load, and with both horizontal shear reinforcement and horizontal load, respectively.

Table A.1 Comparisons between predictions of corbels PA1 and PA2

Corbel	X_{ic} (mm)	Y_{ic} (mm)	Measured shear capacity (kN)	Predicted shear capacity (kN)	% Ratio between predicted and measured
PA1	496	500	550	596	108
PA2	1950	500	800	784	98

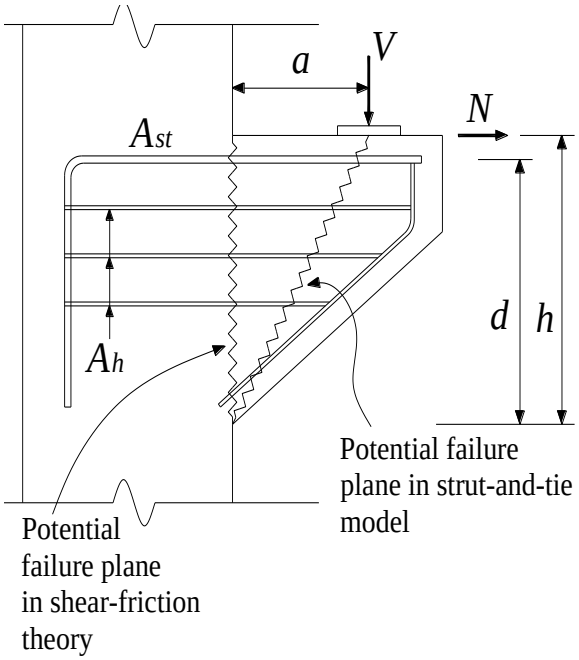

Fig. 1- Potential failure planes of corbels considered in existing models.

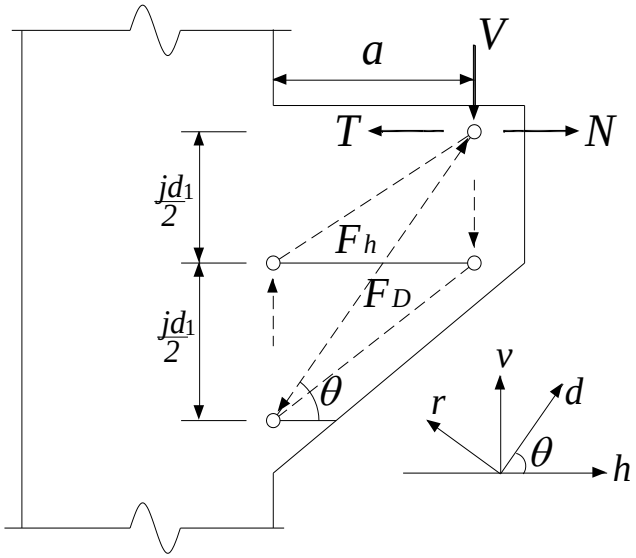

(a) Hwang et al.[11]

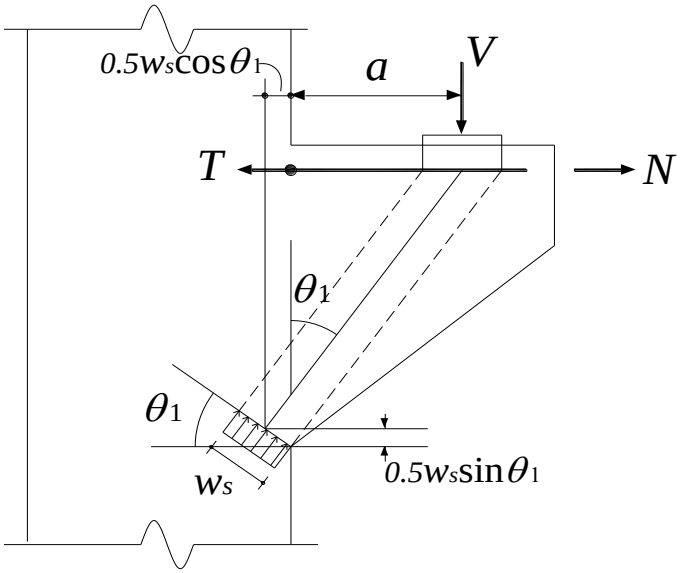

(b) Russo et al.[4]

Fig. 2- Typical strut-and-tie models of corbels

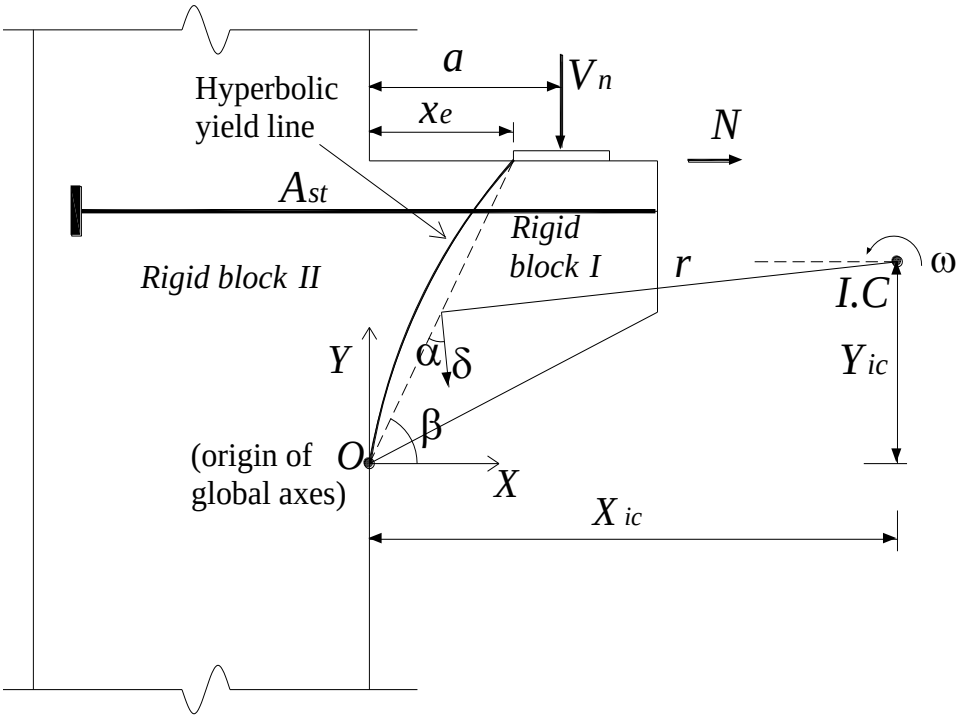

(a) Hyperbolic yield line

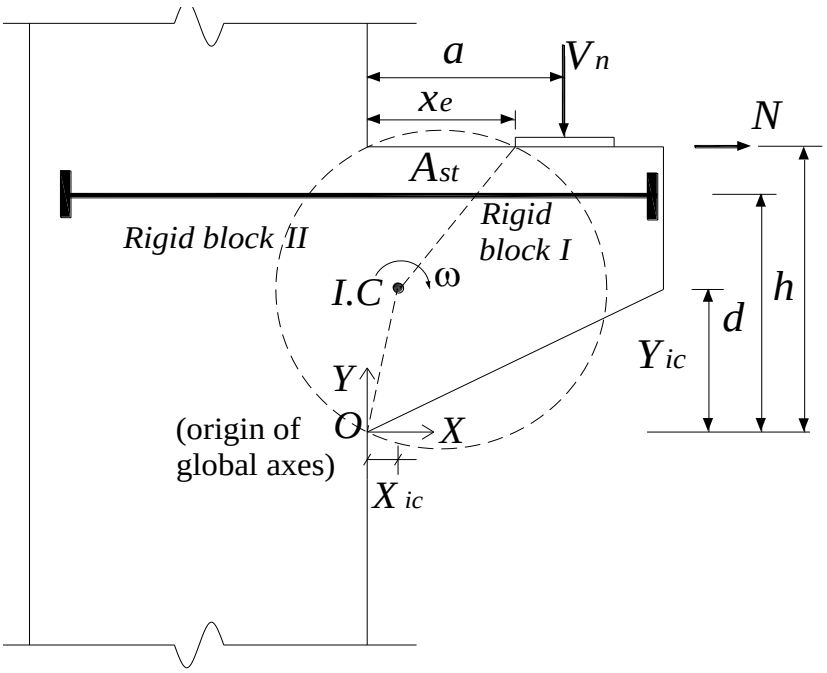

(b) Yield line with two straight segments

Fig. 3- Idealized failure mechanism of corbels.

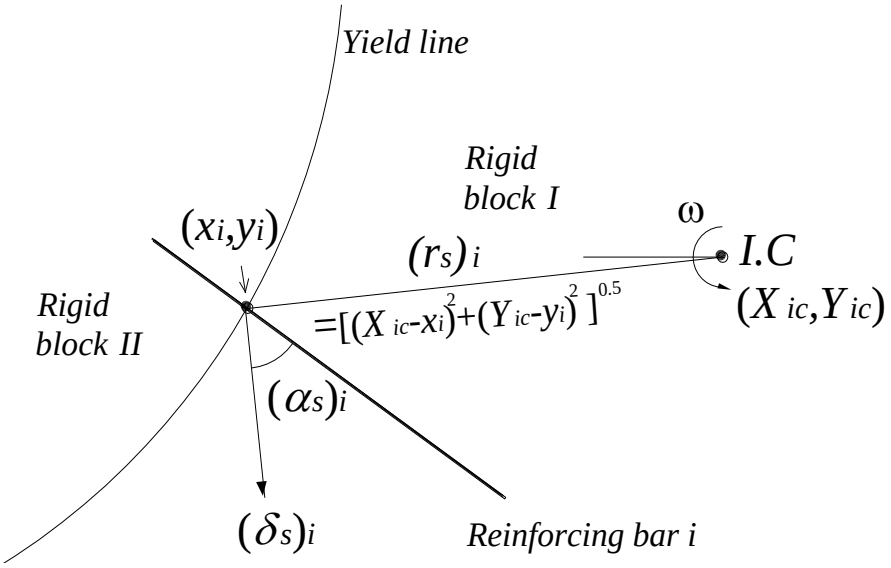

Fig. 4- Reinforcing bar crossing yield line.

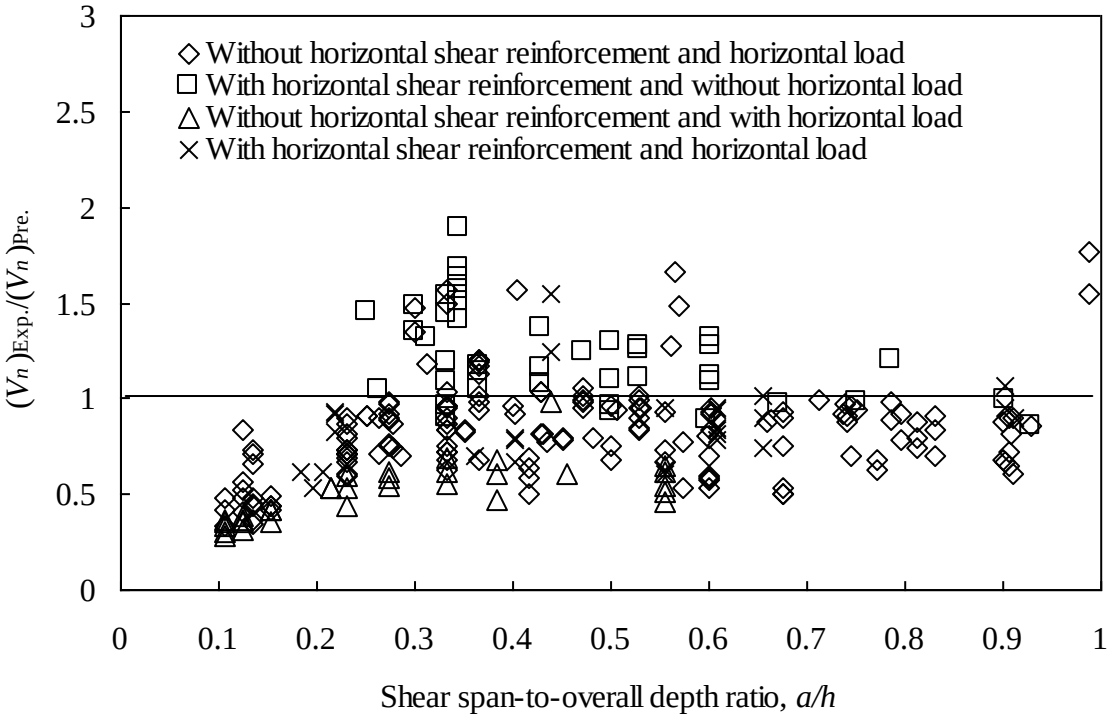

(a) Fattuhi's equation

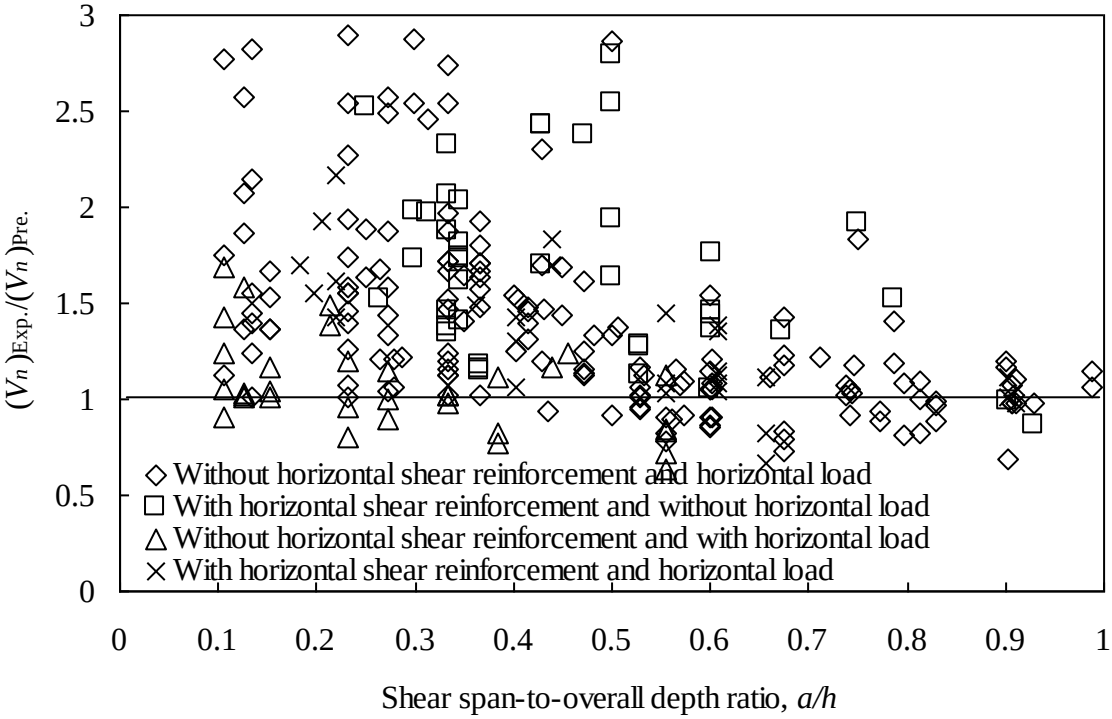

(b) ACI 318-05

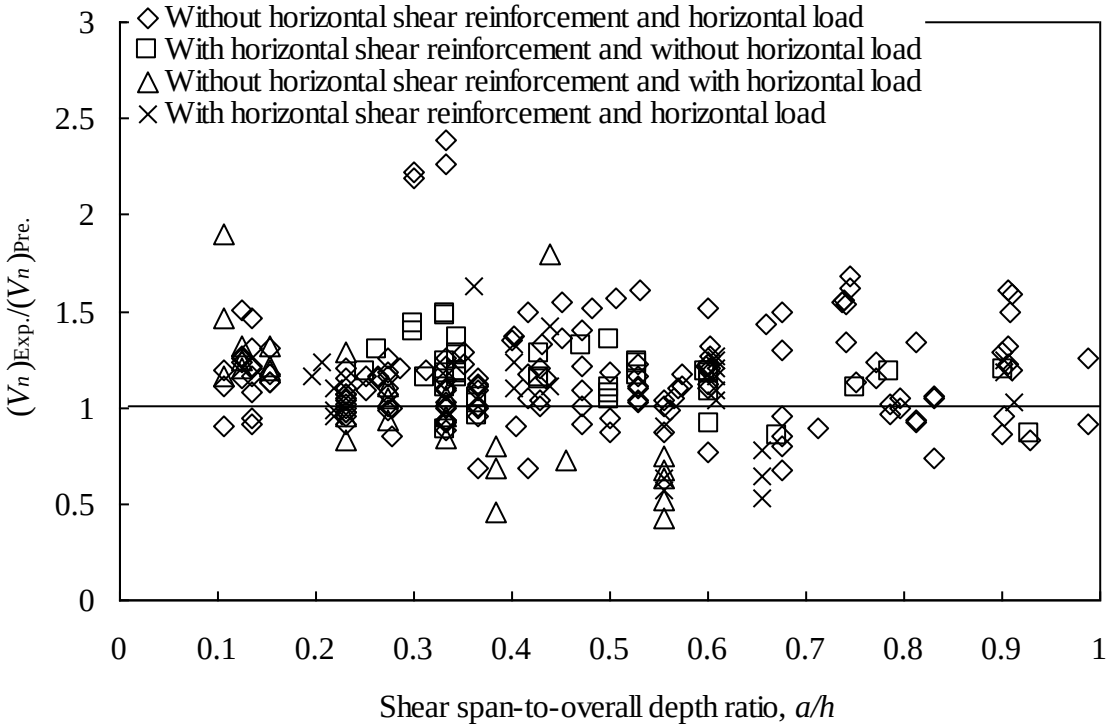

(c) Softened strut-and-tie model by Hwang et al.

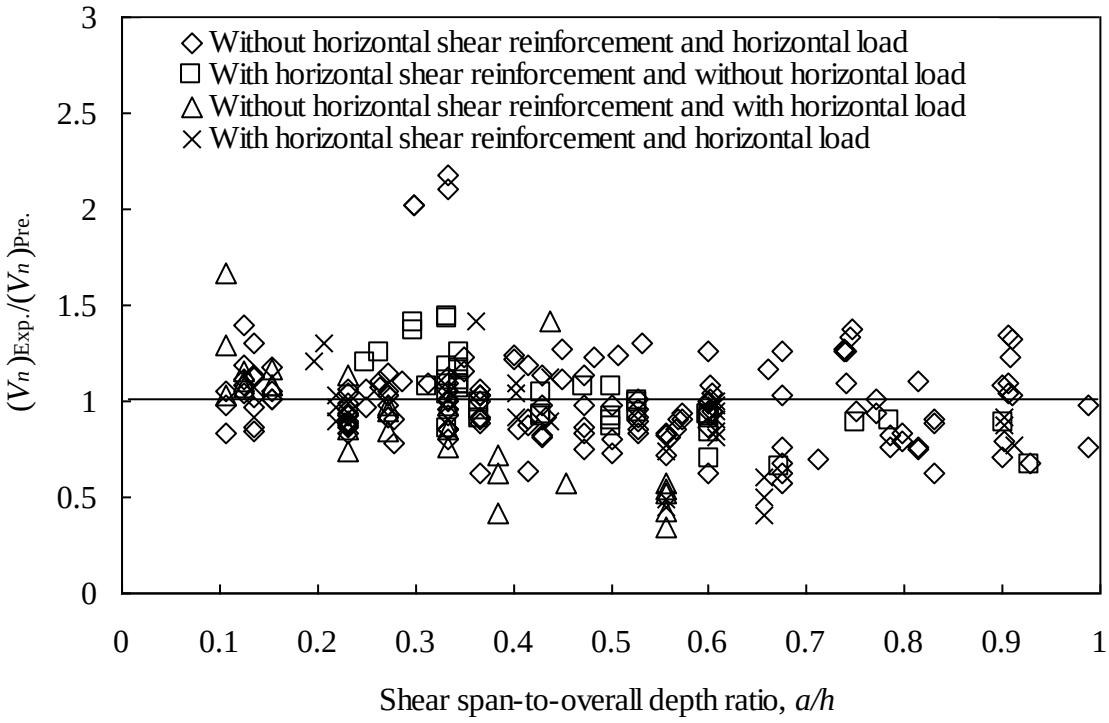

(d) Strut-and-tie model by Russo et al.

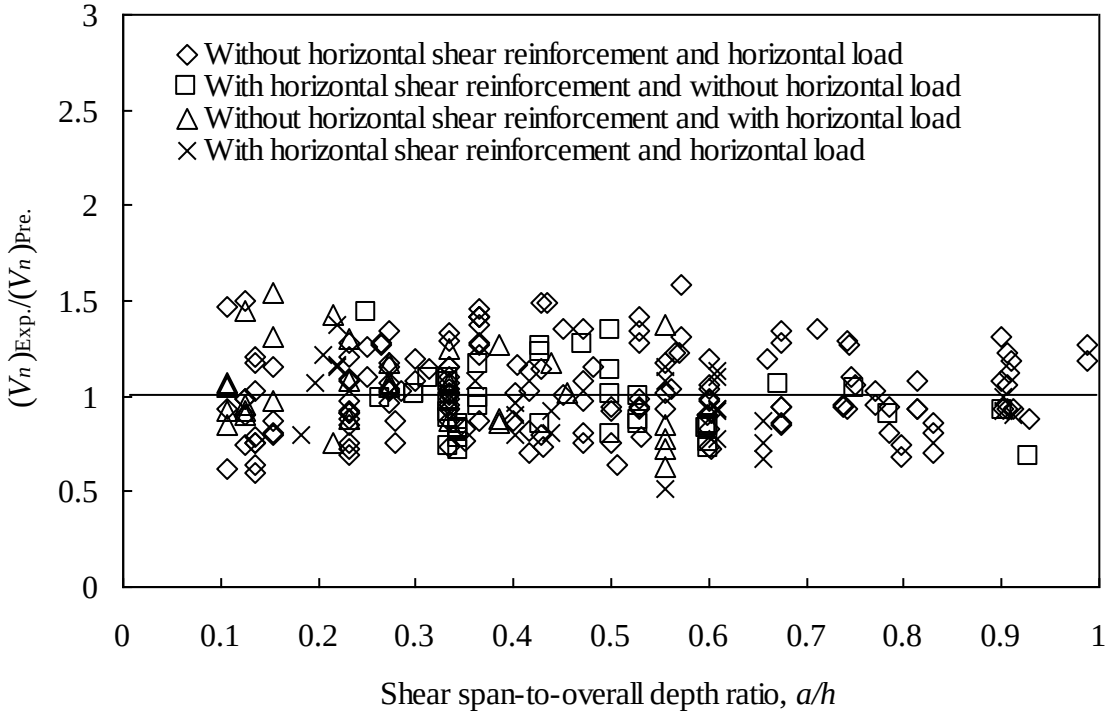

(e) Mechanism analysis

Fig. 5-Comparisons of measured and predicted shear capacities.

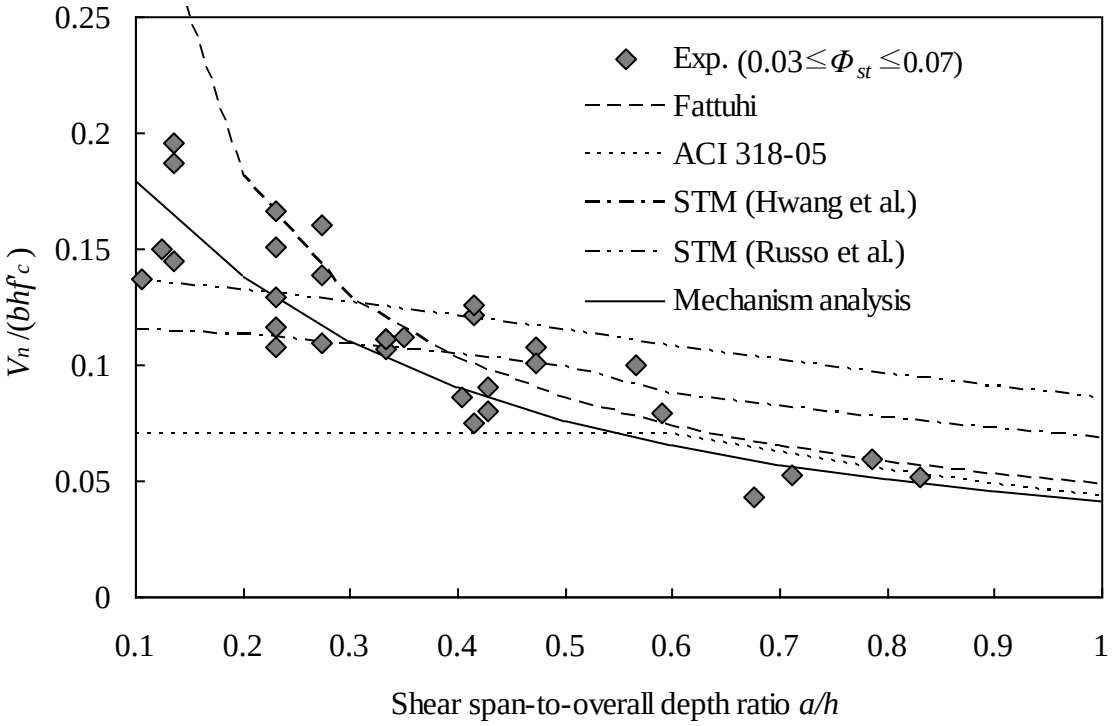

(a) $\phi_{st} = 0.05$

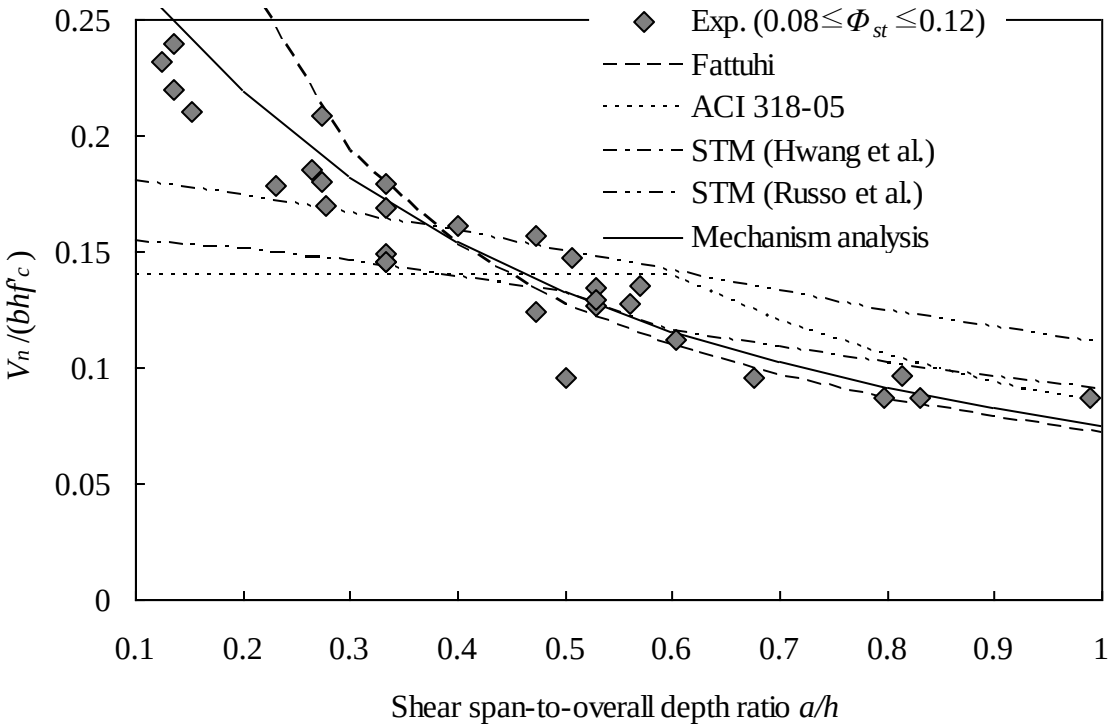

(b) $\phi_{st} = 0.1$

Fig. 6- Influence of a/h on shear capacity of corbels.

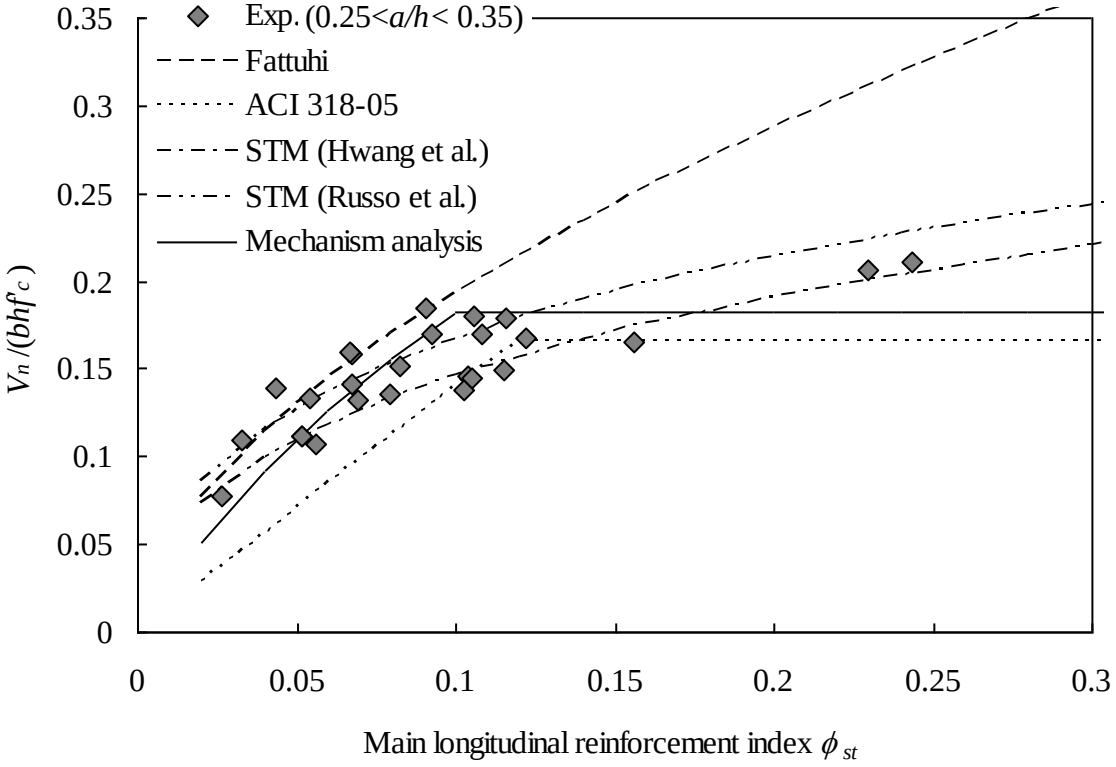

(a) $a/h = 0.3$

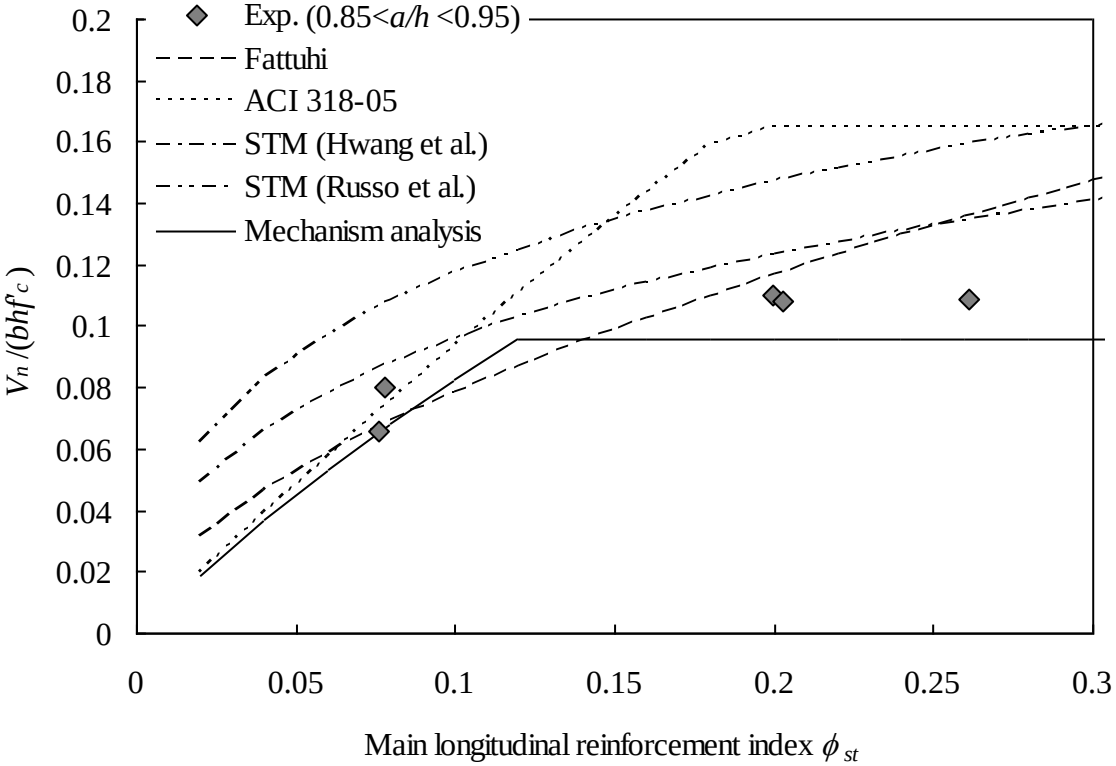

(b) $a/h = 0.9$

Fig. 7- Influence of ϕ_{st} on shear capacity of corbels.

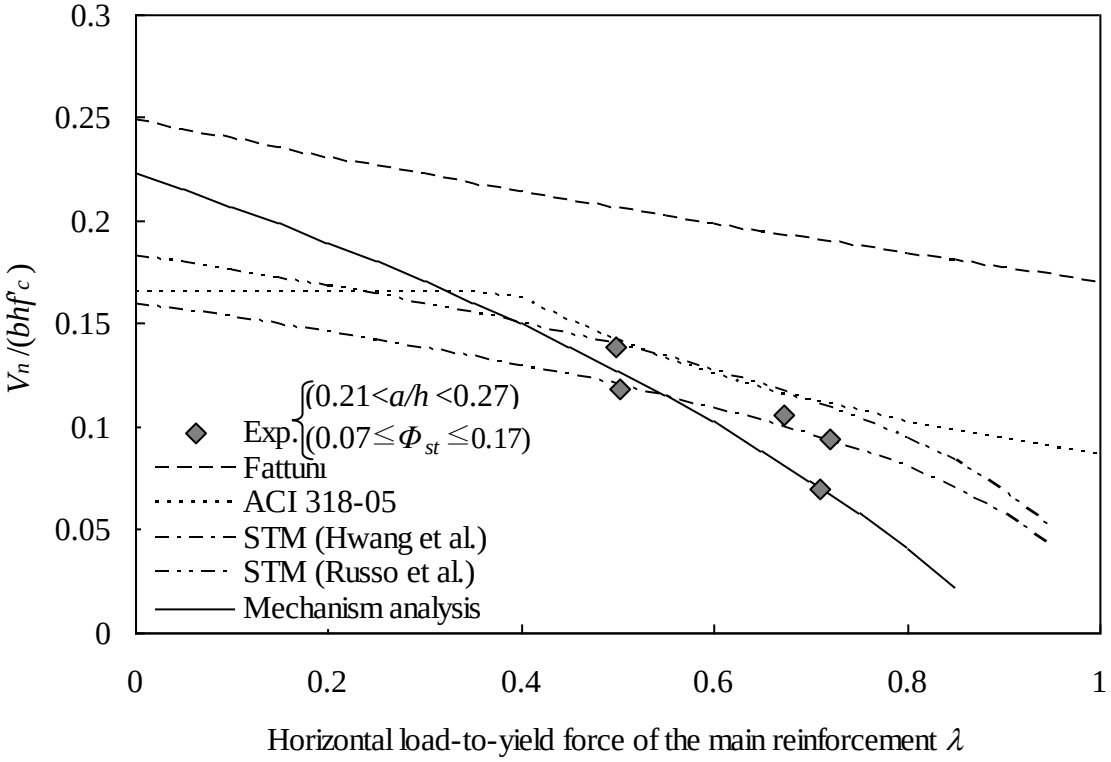

(a) $a/h = 0.25$

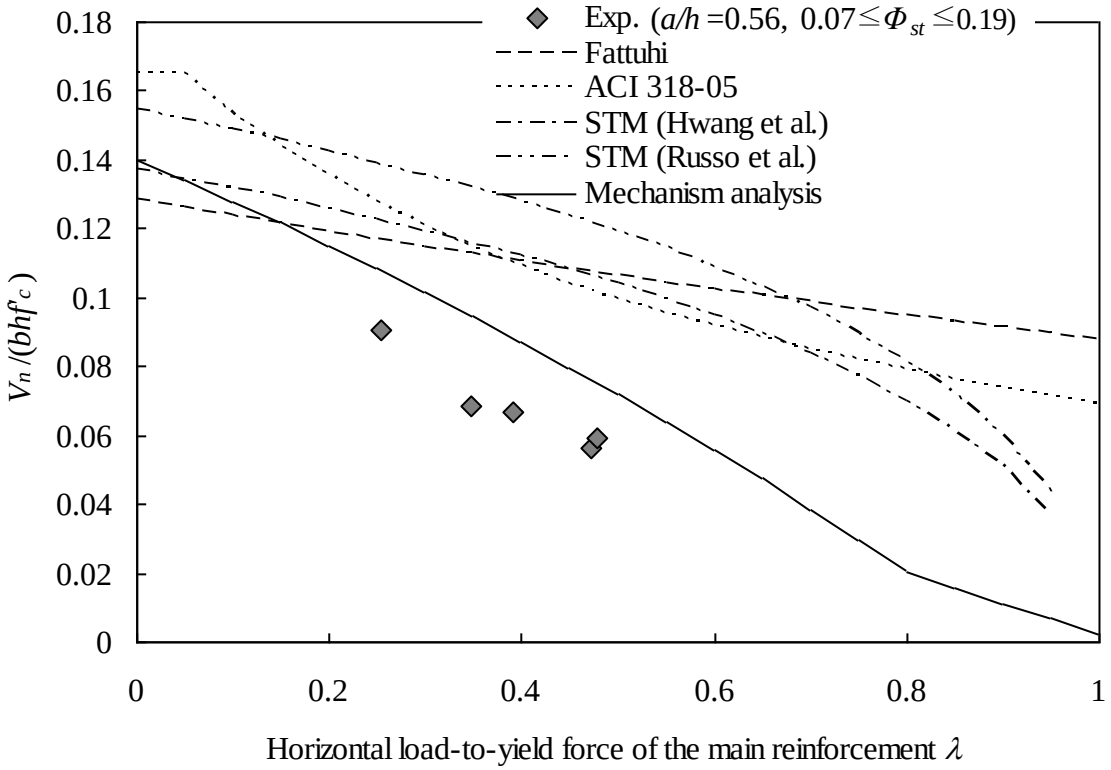

(b) $a/h = 0.56$

Fig. 8- Influence of λ on shear capacity of corbels ($\phi_{st} = 0.12$, $\phi_h = 0$).

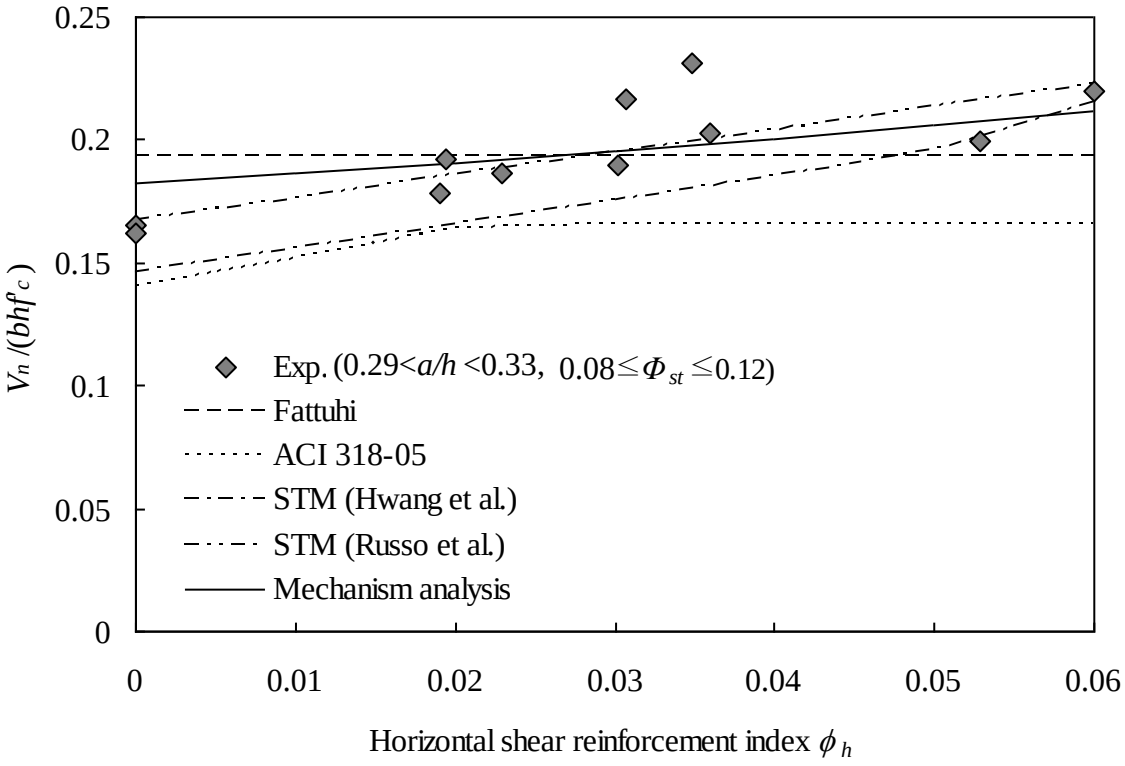

(a) $a/h = 0.3$

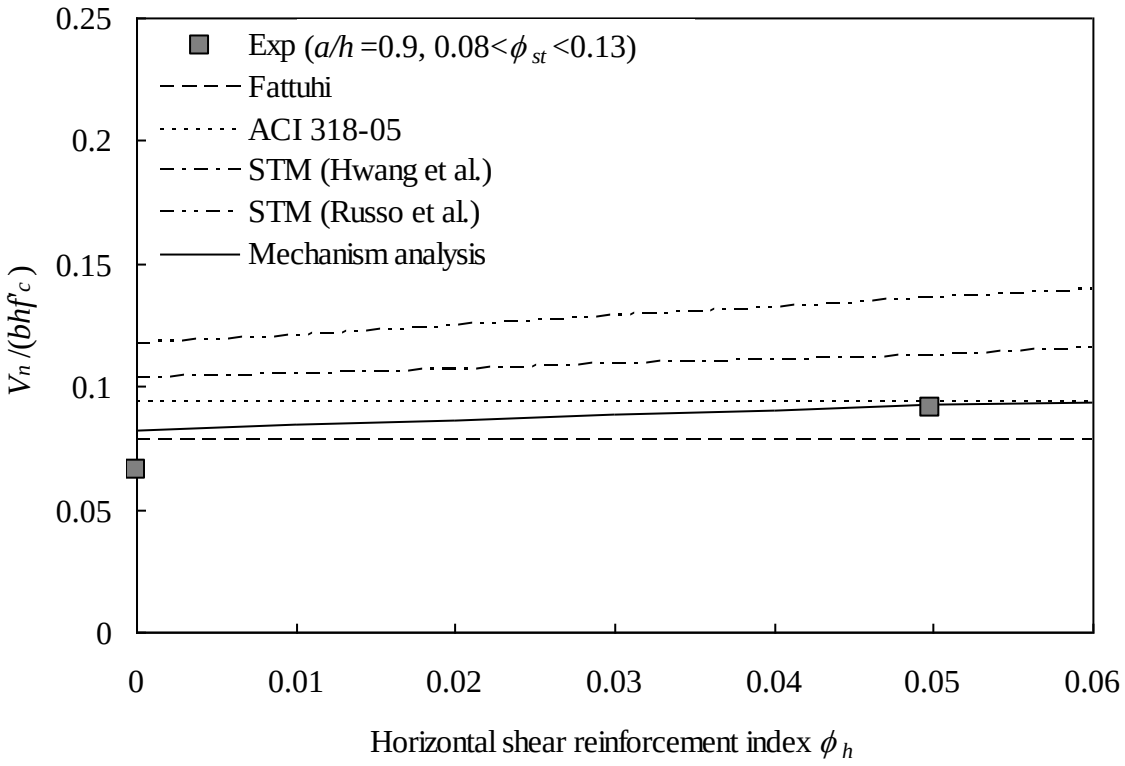

(b) $a/h = 0.9$

Fig. 9- Influence of ϕ_h on shear capacity of corbels ($\phi_{st} = 0.1,\ \lambda = 0$).